Original Article

Enhancement of cytotoxic effects with ALA-PDT on treatment of radioresistant cancer cells

Takafumi Ikeda,[1,†] Hiromi Kurokawa,[1,2,3,†,*] Hiromu Ito,[1,4,*] Kiichiro Tsuchiya,[1] and Hirofumi Matsui[1,2,*]

[1]Faculty of Medicine, University of Tsukuba, 1-1-1 Tennodai, Tsukuba, Ibaraki 305-8575, Japan
[2]Algae Biomass Research and Development, University of Tsukuba, 1-1-1 Tennodai, Tsukuba, Ibaraki 305-8572, Japan
[3]Phycochemy Corp., 2-10-2 Matsushiro, Tsukuba, Ibaraki 305-0035, Japan
[4]Quantum RedOx Chemistry Team, Institute for Quantum Life Science (iQLS), Quantum Life and Medical Science Directorate (QLMS), National Institutes for Quantum Science and Technology (QST), 4-9-1 Anagawa, Inage-ku, Chiba-shi, Chiba 263-8555, Japan

(Received 4 September, 2023; Accepted 25 September, 2023; Released online in J-STAGE as advance publication 3 October, 2023)

Radiation therapy is a lower invasive local treatment than surgery and is selected as a primary treatment for solid tumors. However, when some cancer cells obtain radiotherapy tolerance, cytotoxicity of radiotherapy for cancer cells is attenuated. Photodynamic therapy (PDT) is a non-invasive cancer therapy combined with photosensitizers and laser irradiation with an appropriate wavelength. PDT is carried out for recurrent esophageal cancer patients after radiation chemotherapy and is an effective treatment for radiation-resistant tumors. However, it is not clear why PDT is effective against radioresistant cancers. In this study, we attempted to clear this mechanism using X-ray resistant cancer cells. X-ray resistant cells produce high amounts of mitochondria-derived ROS, which enhanced nuclear translocation of NF-κB, resulting in increased NO production. Moreover, the expression of PEPT1 that imports 5-aminolevulinic acid, the precursor of photosensitizers, was upregulated in X-ray resistant cancer cells. This was accompanied by an increase in intracellular 5-aminolevulinic acid-derived porphyrin accumulation, resulting in enhancement of PDT-induced cytotoxicity. Therefore, effective accumulation of photosensitizers induced by ROS and NO may achieve PDT after radiation therapy and PDT could be a promising treatment for radioresistant cancer cells.

***Key Words*: 5-aminolevulinic acid, PDT, radioresistant cancer, nitric oxide, NF-κB**

The number of patients with cancer is increasing dependent on the proceeding the aging society in the world. Common cancer treatments utilized recently are surgery, radiation therapy, chemotherapy, and immunotherapy. Radiation therapy is a lower invasive local treatment than surgery because of ionizing radiation sensitivity. Thus, radiation therapy is selected as a primary treatment for solid tumors. Moreover, radiosensitivity on tumor is higher than normal tissue.[1] According to this phenomenon, radiation therapy can induce cancer specific cell death without relatively severe side-effects.

Radiation can induce cellular DNA damage directly and indirectly with double strand or single stand DNA breaks.[2] In normal cells, cellular injury caused by radiation can be effectively repaired compared to cancer cells.[3] However, some cancer cells obtain radioresistance and can attenuate damage derived from radiation.[4] Radiotherapy tolerance is one of the most severe problem in cancer therapy and would directly influence the subsequent prognosis.[5]

Photodynamic therapy (PDT) is a cancer therapy that utilizes a combination of photosensitizers and laser.[6] Just after exposure to the light with an optimal wavelength, photosensitizers are excited, and then reactive oxygen species (ROS) is produced immediately through the energy transition reaction.[7] ROS could be a potent cytotoxic and cancer cell death is induced.[8] The phenomenon of cancer-specific uptake of porphyrins was reported in the early 20th century, and PDT came into one of the cancer treatment in the 1970s.[9] Kennedy *et al.*[10] reported that 5-aminolevulinic acid (5-ALA) is utilized in PDT as a heme precursor of protoporphyrin IX (PpIX) in 1992. PpIX accumulation levels in cancer cells are higher than in normal cells because of the metabolic abnormality and expressions of several transporters. Therefore, cancer specific cytotoxicity can be achieved with PDT.

PDT is carried out for recurrent esophageal cancer patients after radiation chemotherapy.[11] From therapeutic outcomes, it is indicated that PDT is an effective treatment for radiation-resistant tumors. However, the mechanism of the effective therapeutic outcomes on the radioresistant cancer cells with PDT is still unclear. In general, radioresistant tumors are reported to produce high amounts of ROS.[12] Thus, the relationship between intracellular ROS production and porphyrin metabolic pathways may influence the intracellular PpIX accumulation and cytotoxic effects with PDT. In this study, we evaluated whether ALA-PDT is an effective treatment for radioresistant tumors.

Materials and Methods

Cell culture. RGK1 cells (RGK-WT) were established by Shimokawa *et al.* by inducing a cancer-like mutation in RGM1 cells, a rat gastric epithelial cell line, was purchased from RIKEN CELLBANK (Ibaraki, Japan).[13] RGK-WT were cultured in Dulbecco's Modified Eagle's Medium/Nutrient Mixture F-12 Ham with 15 mM HEPES and sodium bicarbonate, without L-glutamine, liquid, sterile-filtered (Sigma-Aldrich Co. LLC, St. Louis, MO) with 10% fetal bovine serum (Cytiva, Tokyo, Japan) and 1% penicillin/streptomycin. Cells were cultured at 37°C and 5% CO_2.

X-ray resistant strain. X-ray resistant RGK1 strains (RGK-XRR) were established in our laboratory. X-irradiation was carried out using an X-irradiation system MBR-1505R (Hitachi Power Solutions Co. Ltd., Hitachi, Japan) for 23 days. To maintain the properties of X-ray resistant strains, further X-ray irradiation was performed using another device, MBR-1520R (Hitachi Power Solutions) for more 7 days. The irradiation was performed under the following conditions: tube voltage of 120 kV, tube current of 3.8 mA, and filter of 0.5 mm Al. 2 Gy/day irradiation was performed for a total of 30 days. During 30 days irradiation,

[†]These authors equally contributed to this work.
*To whom correspondence should be addressed.
E-mail: hkurokawa.tt@md.tsukuba.ac.jp (HK); ito.hiromu@qst.go.jp (HI); hmatsui@md.tsukuba.ac.jp (HM)

doi: 10.3164/jcbn.23-79

subculture was performed 3–5 times. Survival cells with this irradiation were designated as X-ray-resistant strains.

Mitochondrial reactive oxygen species (mitoROS) assay. To evaluate mitochondrial ROS production, MitoSOX™ Red superoxide indicator (Thermo Fisher Scientific Inc., Waltham, MA) was used. Cells were seeded at a density of 1×10^4 cells/well in 96-well plates (black plate clear bottom) and cultured overnight. The medium was replaced with HBSS containing 5 μM MitoSOX and incubated at 37°C for 30 min. Fluorescence intensity was measured with a Varioskan microplate reader (Thermo Fisher Scientific Inc.). Fluorescence was excited at 396 nm and measured at 610 nm filter.

Measurement of intracellular NO production. RGK-WT and RGK-XRR were cultured overnight at a density of 5×10^4 cells/well in 6-well plates. After the supernatant aspiration, cells were incubated in FluoroBrite™ DMEM (Thermo Fisher Scientific Inc.) with 10 μM diaminorhodamine-4M acetoxymethyl ester (DAR-4M AM) (Goryo Chemical, Hokkaido, Japan) for 15 min. After incubation, the medium was replaced with FluoroBrite™ DMEM. Fluorescence images were obtained, and the intensity was measured using a fluorescence microscope IX83 (Olympus Optical Co. Ltd., Tokyo, Japan). Fluorescence was excited at 535–555 nm, and emission was observed using a 570–625 nm filter.

Immunohistochemistry of NF-κB. RGK-WT and RGK-XRR were cultured in slide chambers 8 wells. After incubation, cells were incubated with PBS containing 4% paraformaldehyde for 15 min. After aspirating the supernatant, cells were washed three times with PBS and added 0.5% Triton™ X-100 dissolved in PBS, then incubated for 15 min. After treatment, cells were incubated for 60 min in blocking reagent. Anti-rabbit NF-κB antibodies (Genetex Inc., Irvine, CA) (1:1,000) were added to the Can Get Signal Immunoreaction Enhancer Solution 1 (TOYOBO CO., LTD., Osaka, Japan) as a primary antibody and cells were incubated for 1 h. After incubation, cells were washed three times with PBS and Goat anti-Rabbit IgG (H+L) Cross-Adsorbed Secondary Antibody, Alexa Fluor™ 405 (Thermo Fisher Scientific Inc.) (1:1,000), was added to the Can Get Signal Immunoreaction Enhancer Solution 2 (TOYOBO CO., LTD.) and cells were incubated for 1 h using this solution. After treatment, cells were washed three times with PBS and observed under an all-in-one fluorescence microscope (BZ-X710; Keyence Corp., Osaka, Japan).

Measurement of PEPT1 and ABCG2 expression by Western blotting. Protein expression of PEPT1 and ABCG2 in RGK-WT and RGK-XRR was analyzed by Western blotting. The cells were washed three times with PBS and lysed with RIPA buffer (FUJIFILM Wako Pure Chemical Corporation, Osaka, Japan) on ice to make a total cell lysate, then heating at 70°C for 10 min. For SDS-polyaclylamide gel electrophoresis, the cell lysates were added into wells of ePAGEL® E-T12.5L (ATTO Corporation). Gels were electrophoresed at 250 V for 20 min and proteins were transferred to polyvinylidene fluoride (PVDF) membranes (Clear Blot P+ Membrane; ATTO Corporation, Tokyo, Japan). PVDF membranes were blocked with PVDF blocking reagent, Can Get Signal® (TOYOBO CO., LTD.) for 60 min. Anti-PEPT1 antibody (Abcam plc, Cambridge, UK) and anti-ABCG2 antibody (Cell Signaling Technology Japan K.K., Tokyo, Japan) were diluted 1:1,000 in Can Get Signal Immunoreaction Enhancer Solution 1 (TOYOBO CO., LTD.) and were allowed to react with the membrane at 4°C overnight. After aspiration of the primary antibody solution, the membrane was washed three times with PBS containing 0.1% Tween 20 (Sigma-Aldrich Co.) (PBS-T) for 5 min. The secondary HRP-linked anti-rabbit IgG antibody (Cell Signaling Technology Japan K.K.) (1:1,000) was added to Can Get Signal® immunoreaction enhancer solution 2 (TOYOBO, CO., LTD.), to which the membrane was exposed for 60 min. After reaction, the membrane was washed three times with PBS-T. The membrane was reacted with Lumina Forte Western HRP Substrate (Millipore Co., Billerica, MA) and the luminescence was captured and measured on an ImageQuant LAS4000 (GE Health Care Japan, Tokyo, Japan). β-Actin was detected with an anti-β-actin antibody (Cell Signaling Technology Japan K.K.) and was used as a sample loading control.

Measurement of intracellular PpIX fluorescence. RGK-WT and RGK-XRR were seeded at 2×10^4 cells/well in 24-well cell culture plates, respectively, and cultured for overnight. The medium was replaced with 1 mM 5-ALA hydrochloride (FUJIFILM Wako Pure Chemical Corporation) and incubated in the dark for 6 h. After removing the medium and washing three times with PBS, the cells were lysed in 100 μl/well of RIPA buffer and transferred to a 96-well cell culture plate. The fluorescence intensity of the cell lysate was measured with a Synergy H1 microplate reader (BioTek Instruments Inc., Winooski, VT). The wavelength was excited at 415 nm and the fluorescence wavelength at 625 nm was measured.

PDT and cell viability. RGK-WT and RGK-XRR were seeded in 6-well plates at 5×10^5 cells/well and cultured for 2 days. The cells were incubated in medium supplemented with 1 mM 5-ALA hydrochloride for 6 h. The medium was removed and washed 3 times with 1 ml of FluoroBrite™ DMEM (Thermo Fisher Scientific Inc.). After 1 day incubation, the cells were incubated with 0.05% trypsin/EDTA (0.05%) for 1 day. The cells were collected and stained with Trypan Blue Stain [Invitrogen™ Trypan Blue Stain (0.4%)] and measuring cell number using the Countess C10281 automated cell counter (Thermo Fisher Scientific Inc.). Cells were irradiated with laser light (635 nm, 0.5 J/cm^2) for PDT via 3ch LD Light Source & Modulation System (YAMAKI CO., LTD., Tokyo, Japan).

Statistical analysis. Microsoft Excel (Microsoft Corporation, Redmond, WA) or SPSS (IBM Corporation, Armonk, NY) was used for statistical processing; Student's *t* test was used to test between the two groups and Tukey's post-hoc was used to test more than two data sets. *P* value less than 0.05 was considered to be statistically significant. All data are presented as mean ± SD.

Results

Measurement of intracellular mitoROS production. The production of mitoROS in cells was evaluated by detecting the fluorescence of MitoSOX. As shown in Fig. 1, the fluorescence intensity of MitoSOX was predominantly elevated in RGK-XRR compared to the RGK-WT, indicating that increased ROS production from mitochondria in the RGK-XRR was confirmed.

Measurement of intracellular NO production. Intracellular NO production was detected by DAR-4M AM. Intracellular fluorescence intensity was observed under fluorescence microscopy. Intracellular NO production in X-ray resistance RGK-XRR is significantly higher than in RGK-WT (Fig. 2).

Nuclear translocation of NF-κB. NF-κB induces various genes involved in cell survival and inflammatory responses through nuclear translocation and activation.[14] NO and ROS are caused by nuclear translocation of NF-κB.[15,16] Under microscopic observation of immunohistochemical staining, both RGK-XRR and RGK-WT cells showed nuclear expression of NF-κB (Fig. 3A). Nuclear fluorescence intensity in RGK-XRR was significantly higher than in RGK-WT (Fig. 3B). This result indicates that NF-κB expression was more enhanced in RGK-XRR compared to RGK-WT.

Expression of 5-ALA uptake protein and PpIX excretion protein. Western blotting was used to evaluate PEPT1, an uptake protein of 5-ALA, and ABCG2, an excretion protein of PpIX on which PDT acts directly. PEPT1 showed a trend toward increased expression in X-ray resistant strains over RGK-WT.

doi: 10.3164/jcbn.23-79

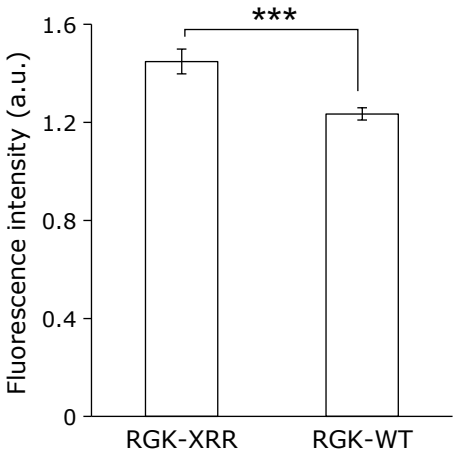

Fig. 1. Intracellular fluorescence intensity of MitoSOX. MitoROS was detected by staining with MitoSOX™ Red superoxide indicator and fluorescence intensity was measured. Fluorescence intensity of MitoSOX was higher in RGK-XRR than in RGK-WT. Data are expressed as mean ± SD (n = 12). Statistical significance was tested with Student's t test. ***p<0.005.

Furthermore, the expression of ABCG2 was significantly upregulated in X-ray resistant strains compared to RGK1. This indicates that both 5-ALA uptake protein and PpIX excretion protein are upregulated in X-ray resistant strains.

Intracellular PpIX accumulation. Quantification of PpIX metabolized and accumulated in the X-ray resistant strains and RGK-WT was performed after 5-ALA administration. Quantification was evaluated by measuring PpIX fluorescence. Fluorescence of PpIX was significantly higher in RGK-XRR than in RGK-WT strain at 6 h after 5-ALA administration, indicating that 5-ALA uptake in RGK-XRR resulted in increased metabolism and accumulation of PpIX.

Effective cytotoxicity of ALA-PDT in RGK-XRR. ALA-PDT was performed on RGK-WT and RGK-XRR. Cell viability was 71.9% in the RGK-XRR with PDT and 85.8% in the RGK-XRR without PDT. 91.9% in the RGK-WT with PDT and 100% in the RGK-XRR without PDT. A significant decrease in cell viability was observed between the RGK-XRR with PDT and RGK-WT with PDT. No significant difference was observed between RGK-WT with and without PDT. In other words, the RGK-XRR was more effective with ALA-PDT than RGK-WT.

Discussion

In this study, we used RGK-WT and RGK-XRR generated from RGK to search for differences in the effects of ALA-PDT

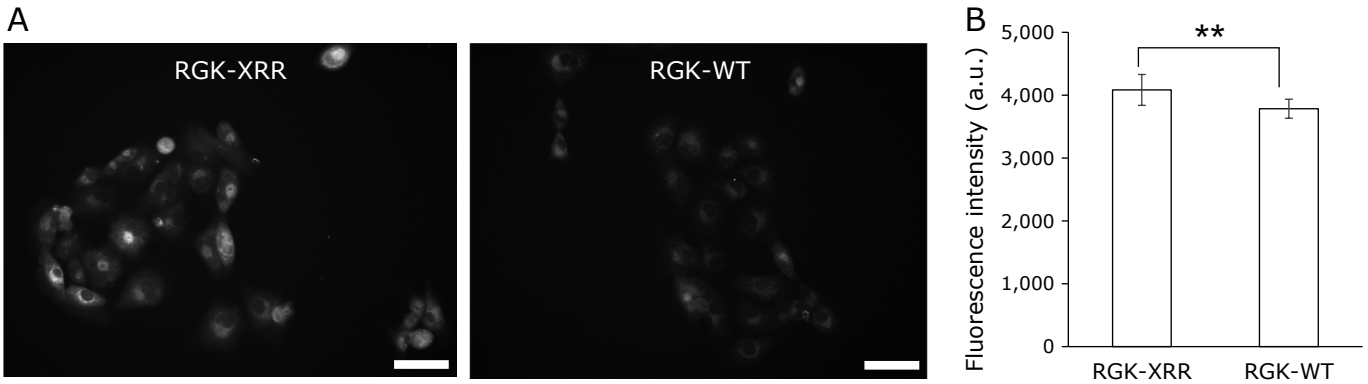

Fig. 2. NO production in RGK-XRR and RGK-WT. (A) Fluorescent microscopy utilized to assess cellular uptake of DAR-4M AM. (B) The fluorescence intensities were analyzed, and the sample size is the number of cells in the analyzed images. Scale bar, 50 μm. Data are expressed as mean ± SD (n = 10). Statistical significance was tested with Student's t test. **p<0.01.

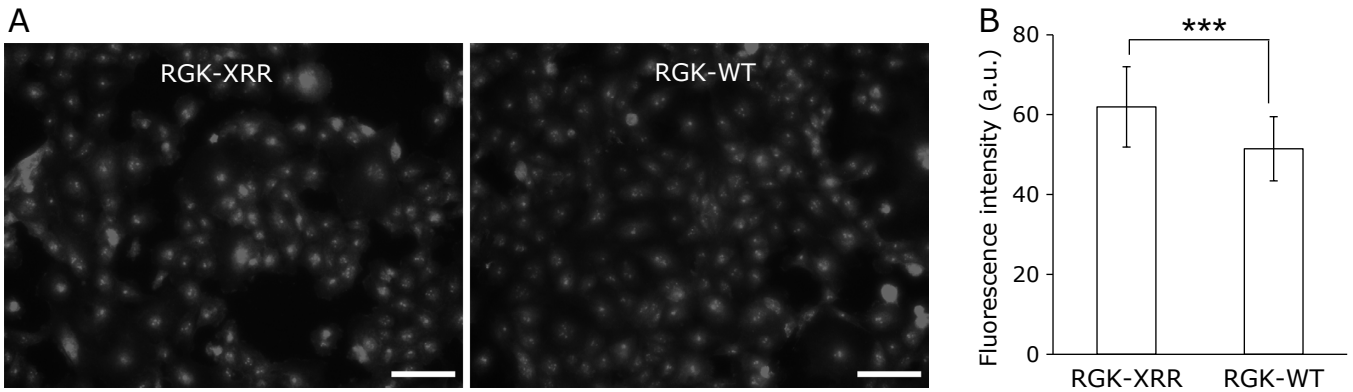

Fig. 3. Immunohistochemistry of NF-κB. (A) Fluorescent microscopy utilized to assess cellular uptake of NF-κB. (B) The fluorescence intensities were analyzed and the sample size is the number of cells in the analyzed images. Scale bar, 100 μm. Data are expressed as mean ± SD (n = 15). Statistical significance was tested with Student's t test. ***p<0.005.

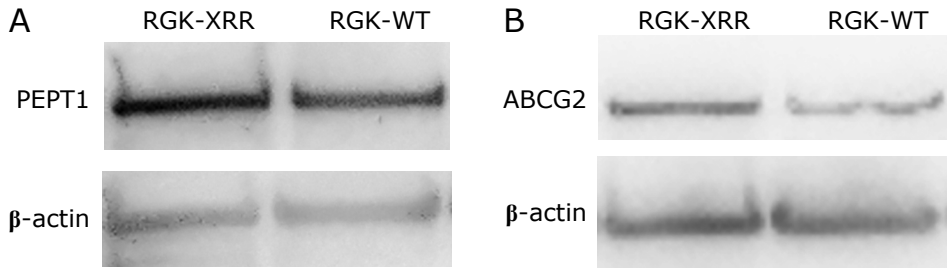

Fig. 4. Representative blotting band images. (A) PEPT1 and β-actin expression. (B) ABCG2 and β-actin expression.

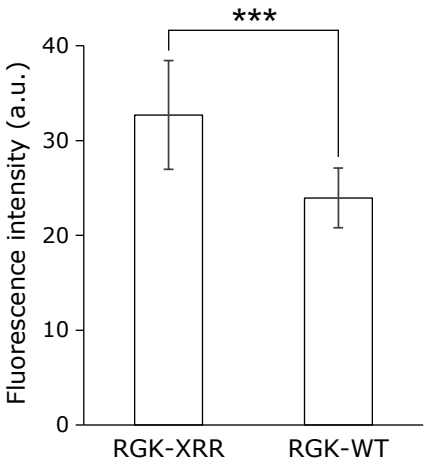

Fig. 5. Comparison of PpIX accumulation. The fluorescence intensity of PpIX was measured with a plate reader. The excitation and emission wavelengths were 415 nm and 625 nm, respectively. Data are expressed as mean ± SD (n = 12). Statistical significance was tested with Student's t test. ***p<0.005.

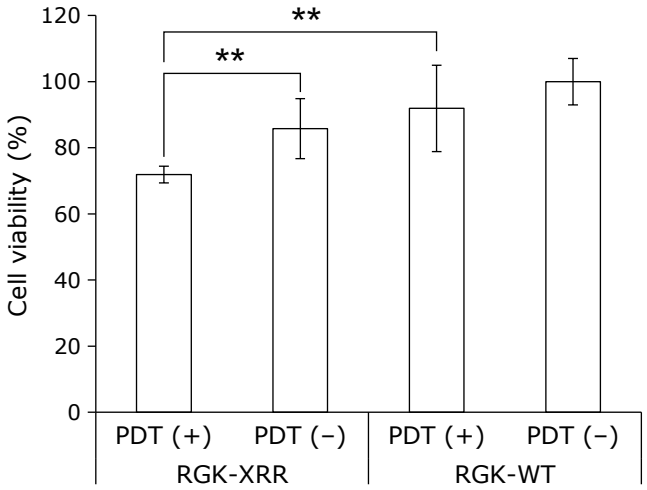

Fig. 6. Cytotoxic effect by ALA-PDT. Cells were stained with Trypan Blue after ALA-PDT. Live and dead cells were measured and cell viability was determined. Data are expressed as mean ± SD (n = 3). Statistical significance was tested with Tukey's post-hoc. **p<0.01.

and the factors that determine these effects. Comparison of the radioresistant strain and the parental strain will help to clarify the factors of radioresistance and is useful for obtaining basic knowledge of cancer cells.[17]

It is reported that X-ray irradiation induces the elevation of intracellular ROS production, and we demonstrated that ROS generation derived from mitochondria increased in the RGK-XRR established by the continual irradiation of X-ray, as shown in Fig. 1. In addition, intracellular production of NO is enhanced through the expression of NO synthase (NOS), and inducible NO synthase (iNOS) is activated via ROS production. In fact, intracellular NO production was increased in RGK-XRR compared to RGK-WT cells, as shown in Fig. 2. Thus, increase of NO generation in the present study was likely to be induced by iNOS activation through the ROS signal transduction.

Intracellular mitoROS and NO production in both cells were evaluated and were higher in the RGK-XRR than in RGK-WT. MitoROS activate NF-κB.[15] Translocation into the nucleus of NF-κB induced iNOS expression and NO production.[16] According to the immunohistochemistry result, NF-κB nuclear localization was more enhanced in RGK-XRR than in RGK-WT (Fig. 3). From these results, MitoROS production was increased and accelerated NF-κB nuclear localization in RGK-XRR. And then, intracellular NO production was increased by upregulation of iNOS expression.

We hypothesized that cytotoxicity of PDT in RGK-XRR would be enhanced compared to the parental RGK-WT because mitoROS and NO production in RGK-XRR increased. We reported that mitoROS can enhance the expression of heme carrier protein 1 (HCP1) and PEPT1.[18,19] HCP1 is carrier protein of heme and porphyrin. PEPT1 is carrier protein of ALA and amino acid. We also reported that the expression of iNOS, which is downstream of mitoROS, induced the increase of NO production and then HCP1 expression was enhanced.[20] From these phenomena, we expected PEPT1 expression was also upregulated by enhancement of NO production. In fact, PEPT1 expression was enhanced through the increase of NO production. We reported that the expressions of ATP-binding cassette sub-family G member 2 (ABCG2), which exports porphyrins and some anti-cancer drugs from cells, were decreased by the upregulation of ROS production.[21] We expected that the ABCG2 expression in the X-ray resistant cells also downregulated because intracellular ROS production increased in the cells. However, the ABCG2 expression in RGK-XRR was higher than in RGK-WT. Thus, several signaling pathways in RGK-XRR might be activated and then the ABCG2 expression upregulated. Some X-ray resistant cells acquired the property of resistance to anti-cancer drugs like doxorubicin, which exports from cells through ABCG2.[22] Indeed, the ABCG2 expression in RGK-XRR was upregulated.

We hypothesized that the upregulation of PEPT1 expression increased the uptake of ALA and enhanced the cytotoxicity of PDT. Compared to RGK-WT, the amounts of intracellular PpIX derived from ALA increased in RGK-XRR 6 h after ALA addition. According to this phenomenon, the effect of PDT was also enhanced.

doi: 10.3164/jcbn.23-79

Although the ABCG2 expression upregulated in RGK-XRR, PpIX accumulation in RGK-XRR also increased and then cytotoxicity of PDT enhanced. We considered intracellular ferrochelatase was inactivated by increase of NO production. NO enhances the effects of ALA-PDT by decreasing the levels of mitochondrial iron-containing enzymes.[23] In other words, when NO is increased, the activity of ferrochelatase is decreased. Thus, PpIX accumulation increases, which may be advantageous in the therapeutic effect of ALA-PDT.

The department of gastroenterology in University of TSUKUBA hospital, PDT was demonstrated for treatment of recurrent esophageal cancer after chemoradiotherapy (CRT). This post-CRT recurrent esophageal cancer is thought to be cancer cells that are resistant to radiation and chemotherapy. The results of this study indicate that PDT is the optimal treatment for salvage treatment of cancer recurrence after radiotherapy. The advantage of this treatment is an effective curative treatment for patients who cannot undergo other invasive treatments. As side effects of PDT, photosensitivity and delirium were reported. However, benefit may be higher for patients with raio- and/or chemo-resistant cancer.

In conclusion, intracellular ROS and NO production in the X-ray resistant cells was higher than in RGK-WT. These indicates that upregulation of PEPT1 expression increases PpIX accumulation derived from ALA and the subsequent enhancement of the cytotoxicity by PDT. Moreover, inactivation of ferrochelatase also contributes to the increased accumulation of PpIX.

Conflict of Interest

No potential conflicts of interest were disclosed.

References

1 Bernier J, Hall EJ, Giaccia A. Radiation oncology: a century of achievements. *Nat Rev Cancer* 2004; **4**: 737–747.
2 Baskar R, Lee KA, Yeo R, Yeoh KW. Cancer and radiation therapy: current advances and future directions. *Int J Med Sci* 2012; **9**: 193–199.
3 Begg AC, Stewart FA, Vens C. Strategies to improve radiotherapy with targeted drugs. *Nat Rev Cancer* 2011; **11**: 239–253.
4 Seo YS, Ko IO, Park H, *et al*. Radiation-induced changes in tumor vessels and microenvironment contribute to therapeutic resistance in glioblastoma. *Front Oncol* 2019; **9**: 1259.
5 Windholz F. Problems of acquired radioresistance of cancer: adaptation of tumor cells. *Radiology* 1947; **48**: 398–404.
6 Dougherty TJ, Gomer CJ, Henderson BW, *et al*. Photodynamic therapy. *J Natl Cancer Inst* 1998; **90**: 889–905.
7 Juarranz A, Jaén P, Sanz-Rodríguez F, Cuevas J, González S. Photodynamic therapy of cancer. Basic principles and applications. *Clin Transl Oncol* 2008; **10**: 148–154.
8 Dolmans DEJGJ, Fukumura D, Jain RK. Photodynamic therapy for cancer. *Nat Rev Cancer* 2003; **3**: 380–387.
9 Dougherty TJ, Kaufman JE, Goldfarb A, Weishaupt KR, Boyle D, Mittleman A. Photoradiation therapy for the treatment of malignant tumors. *Cancer Res* 1978; **38**: 2628–2635.
10 Kennedy JC, Pottier RH. Endogenous protoporphyrin IX, a clinically useful photosensitizer for photodynamic therapy. *J Photochem Photobiol B* 1992; **14**: 275–292.
11 Yano T, Minamide T, Takashima K, Nakajo K, Kadota T, Yoda Y. Clinical practice of photodynamic therapy using talaporfin sodium for esophageal cancer. *J Clin Med* 2021; **10**: 2785.
12 Ewing D, Jones SR. Superoxide removal and radiation protection in bacteria. *Arch Biochem Biophys* 1987; **254**: 53–62.
13 Shimokawa O, Matsui H, Nagano Y, *et al*. Neoplastic transformation and induction of H^+,K^+-adenosine triphosphatase by *N*-methyl-*N'*-nitro-*N*-nitrosoguanidine in the gastric epithelial RGM-1 cell line. *In Vitro Cell Dev Biol Anim* 2008; **44**: 26–30.
14 Lawrence T. The nuclear factor NF-κB pathway in inflammation. *Cold Spring Harb Perspect Biol* 2009; **1**: a001651.
15 Park J, Choi H, Min JS, *et al*. Mitochondrial dynamics modulate the expression of pro-inflammatory mediators in microglial cells. *J Neurochem* 2013; **127**: 221–232.
16 Morris KR, Lutz RD, Choi HS, Kamitani T, Chmura K, Chan ED. Role of the NF-κB signaling pathway and κB cis-regulatory elements on the IRF-1 and iNOS promoter regions in mycobacterial lipoarabinomannan induction of nitric oxide. *Infect Immun* 2003; **71**: 1442–1452.
17 Kuwahara Y, Tomita K, Takabatake T, *et al*. Clinically relevant radioresistant cells; past history and future plans. *J Tohoku Med Pharm Univ* 2019; **66**: 19–24.
18 Ito H, Matsui H, Tamura M, Majima HJ, Indo HP, Hyodo I. Mitochondrial reactive oxygen species accelerate the expression of heme carrier protein 1 and enhance photodynamic cancer therapy effect. *J Clin Biochem Nutr* 2014; **55**: 67–71.
19 Ito H, Tamura M, Matsui H, Majima HJ, Indo HP, Hyodo I. Reactive oxygen species involved cancer cellular specific 5-aminolevulinic acid uptake in gastric epithelial cells. *J Clin Biochem Nutr* 2014; **54**: 81–85.
20 Kurokawa H, Ito H, Terasaki M, *et al*. Nitric oxide regulates the expression of heme carrier protein-1 via hypoxia inducible factor-1α stabilization. *PLoS One* 2019; **14**: e0222074.
21 Kurokawa H, Ito H, Terasaki M, Matsui H. Hyperthermia enhances photodynamic therapy by regulation of HCP1 and ABCG2 expressions via high level ROS generation. *Sci Rep* 2019; **9**: 1638.
22 Kuwahara Y, Roudkenar MH, Suzuki M, *et al*. The involvement of mitochondrial membrane potential in cross-resistance between radiation and docetaxel. *Int J Radiat Oncol Biol Phys* 2016; **96**: 556–565.
23 Yamamoto F, Ohgari Y, Yamaki N, *et al*. The role of nitric oxide in δ-aminolevulinic acid (ALA)-induced photosensitivity of cancerous cells. *Biochem Biophys Res Commun* 2007; **353**: 541–546.